Westfälische Wilhelms-Universität Münster

Otto Creutzfeldt Center for Cognitive and Behavioral Neuroscience

Formation of face-related predictions: An interplay of pre-stimulus alpha/beta enhancement and peri-stimulus N170 diminution

Marlen A. Roehe[1,2], Daniel S. Kluger[2,3], Svea C. Y. Schroeder[1,2], Lena M. Schliephake[1], Jens Boelte[1,2], Axel Kohler[4], Ricarda I. Schubotz[1,2,5]

[1]Department of Psychology, University of Muenster, Germany
[2]Otto Creutzfeldt Center for Cognitive and Behavioral Neuroscience, University of Muenster, Germany
[3]Institute for Biomagnetism and Biosignal Analysis, University of Muenster, Germany
[4]Goethe Research Academy for Early Career Researchers, University of Frankfurt, Germany
[5]Department of Neurology, University Hospital Cologne, Germany

Background

Our environment confronts us with a highly dynamic nature, veiling a cascade of statistical regularities. Explicitly, these regularities often go unnoticed whilst traces of implicit learning are evident in the brain's neural activity[1]. Recent perspectives have offered evidence that both pre-stimulus oscillations and peri-stimulus event-related potentials are reliable biomarkers of implicit expectation arising from statistical learning:

- **N170**: a diminution in amplitude of this face-sensitive event-related potential has been deemed a reliable indicator, highlighting the expectedness of a given face[2].
- **Alpha/Beta oscillations (10 – 15 Hz)**: these low-frequencies mediate the transmission of 'top-down' expectations. An enhancement in alpha/beta power preceding the onset of a stimulus would subsequently classify the stimulus as somewhat expected[3,4,5]. Furthermore, alpha oscillations have been found to boost the precision of prediction errors (via attention) as well as regulate the precision of top-down predictions (via expectation)[6,7].
- **Gamma oscillations (30 – 100 Hz)**: these high-frequencies have been predominantly associated with the transmission of 'bottom-up' sensory driven information and prediction errors[3,8].

Objectives

The central focus of this study was to elucidate the genesis and development of implicit expectations. Hence, our aims were to:

1. Define a timeframe marking the on- and offset of face-related expectation formation.
2. Determine the spectral composition and power distribution pattern illustrating the development of face-related expectations within the previously established timeframe.

Hypotheses

Behavioural

- **H1:** A significant increase in accuracy and decrease in response time for statistically expected vs random face images.

ERP

- **H2:** A significant reduction in the N170 amplitude for expected in comparison to random face images.

Time-frequency

- **H3:** A significant enhancement in gamma band activity (GBA) upon depiction of random face images.
- **H4:** A significant enhancement in alpha/beta power prior to the onset of expected face images.

Materials and Methods

Participants

- 35 right-handed participants (25 ♀; 23.1 ± 3.39 years).

Stimuli

- 25 neutral face images (12 female) chosen from the Radboud Faces Database (RaFD)[19].
- Eight of these images were sorted into four reoccurring pairs.
- Pairs were counterbalanced across participants.

Task

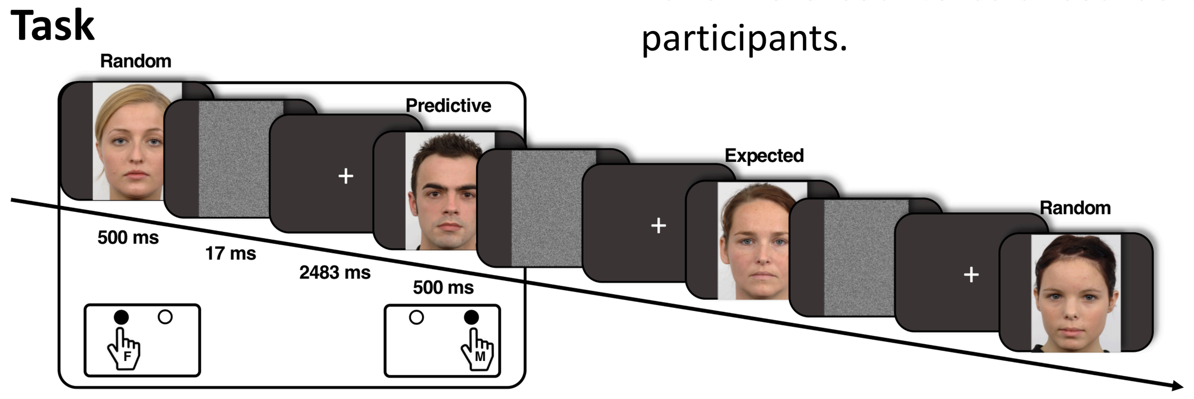

Fig 1. Schematic illustration of the experimental task. Each image was depicted for 500 milliseconds (ms) followed by a white noise mask (17 ms) and a darkened fixation screen (2483 ms). The participants were instructed to press either the left or right button with their right index or middle finger in order to discriminate between female (F) and male (M) images, respectively.

Procedure

- Day 1: **Training** - behavioural, 18-minute statistical learning task (gender classification 'cover-up' task).
- Day 2: **EEG session -** an elongated version of the task encountered the previous day (50 minutes).
  Questionnaire - tested participants' explicit awareness of the predictive nature underlying the task at hand.

EEG Data acquisition

- 62 Ag/AgCl-electrodes in addition to 2 EOGs.
- Online bandpass filtered (0.1 – 1000 Hz) and a sample rate of 1 kHz.
- FCz and FPz served as online reference and ground, respectively.

ERP: Data processing and analysis

- Offline bandpass filtered (0.1 – 30 Hz), corrected for ocular-artefacts, segmented from -200 – 600 ms (locked to image onset), semi-automatic artefact removal and referenced to a common average.
- N170: expected and random image trials were subjected to one-sided, dependent cluster permutation tests with 5000 random iterations across the timeframe of 150 – 200 ms.

TFA: Data processing and analysis

- Offline bandpass filtered (0.5 – 100 Hz), corrected for ocular-artefacts, segmented from -2000 – 1250 ms (locked to image onset), semi-automatic artefact removal and referenced to a common average.
- Consecutive epochs overlapped by 250 ms to minimise loss of data during fast Fourier Transform (500 ms fixed Hanning window).
- **Alpha/Beta** – A Hanning taper was used for frequencies 2 – 30 Hz. A 500 ms fixed sliding window moved in steps of 50 ms and 1 Hz (new time-windows extended from -1.75 to 1 s, stimulus locked).
- **Gamma** - A DPSS multitaper was used for frequencies 30 – 100 Hz; a 500 ms fixed sliding window with identical stepwise motion as above.
- For time-frequency representations (TFRs), one-sided, dependent cluster-based permutation tests (Monte Carlo randomisation tests, 1000 iterations) were used.

Results

Implicit Expectations

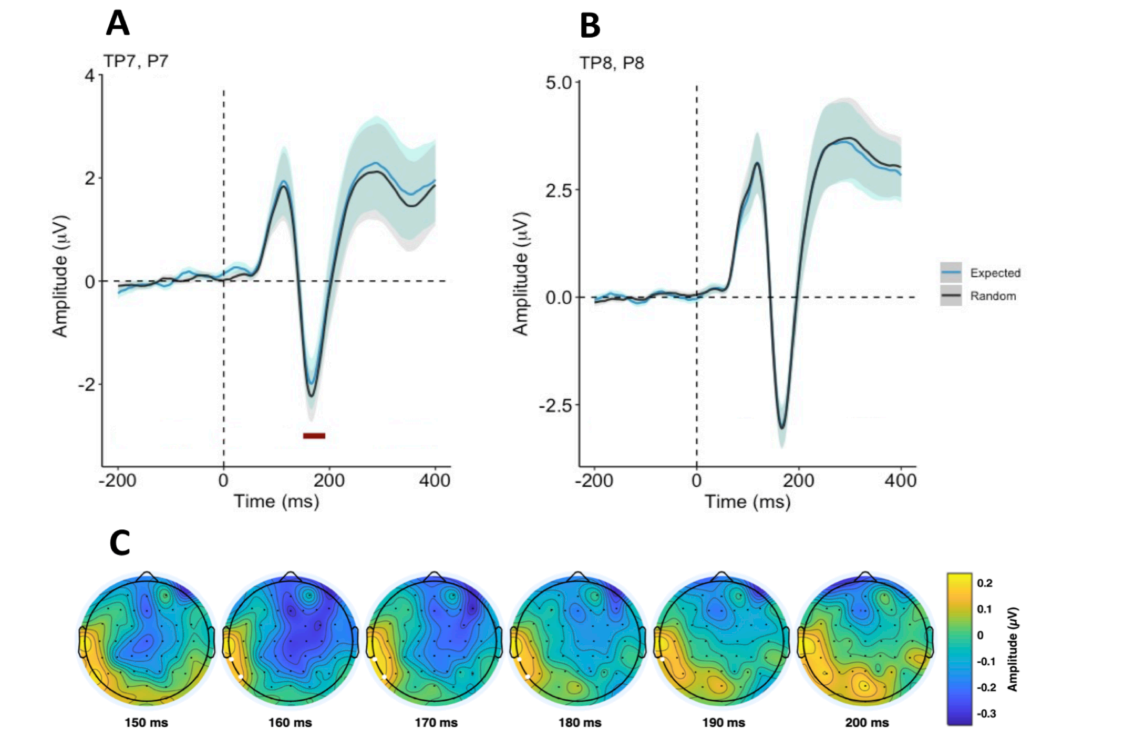

Figure 2. (A) A significant reduction in the N170 amplitude for expected (blue line) vs random (black line) faces was found across the averaged electrodes TP7 and P7 (left hemisphere; p = .003, cluster corrected). The significant timeframe is marked by a dark red dash (152 – 192 ms). The shaded area illustrates within-participants confidence intervals for the expected (blue) and random (grey) faces. **(B)** The N170 illustrates no significant amplitude differences between the image categories across electrodes TP8 and P8 (right hemisphere; p >. 05, cluster corrected). **(C)** The topographies display the voltage difference (μV) between the expected and random face images in a timeframe from 150 to 200 ms after stimulus onset. A significant left-lateralised difference in amplitude extends from approx. 160 – 190 ms post-stimulus onset (electrodes highlighted in white).

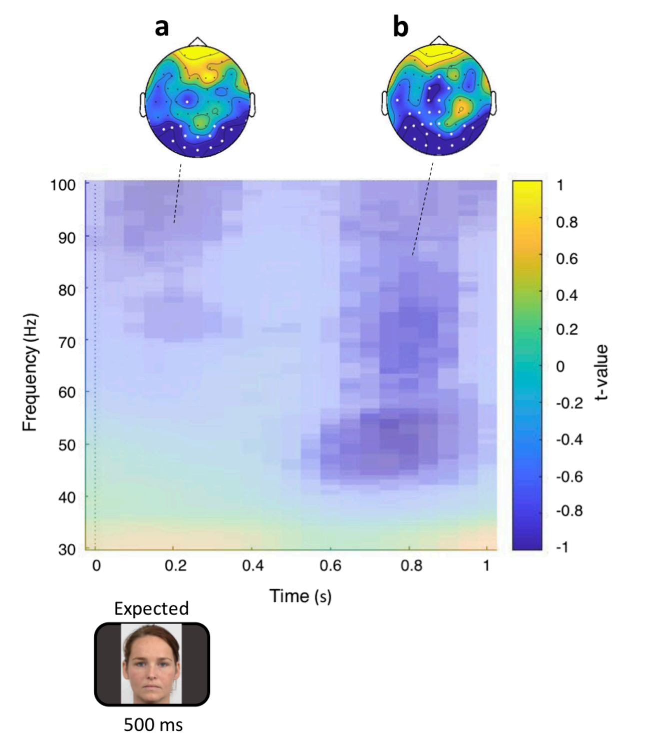

Figure 3. Time-frequency representation (TFR) of the difference in GBA (30 – 100 Hz) between expected and random images during the post-stimulus onset timeframe. Scalp topographies illustrate that primarily posterior distributed channels (highlighted in white) contributed to the negative cluster (p = .041). The t-values were averaged across **(a)** 0 – 0.4 s for the topography depicting the early subcluster (peri-stimulus) and **(b)** 0.4 – 1 s for the topography of the later subcluster.

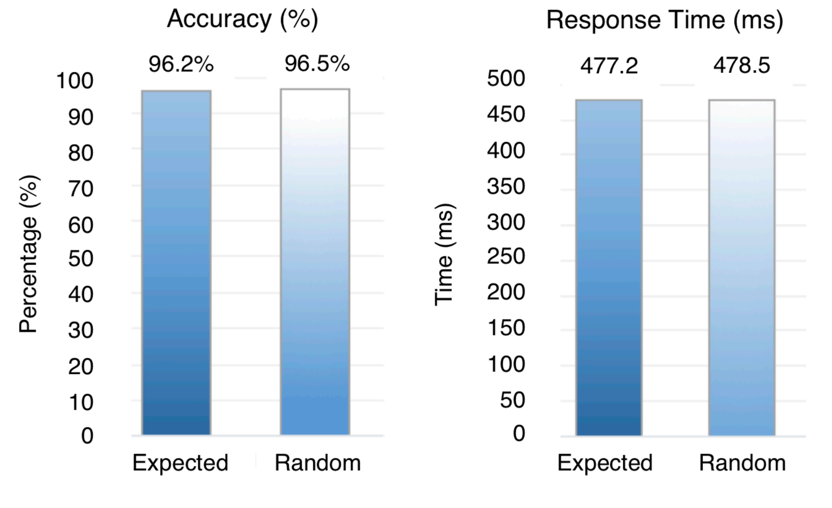

Figure 4. No significant behavioural differences were evident between statistically expected and randomly occurring images.

Implicit Expectation Genesis

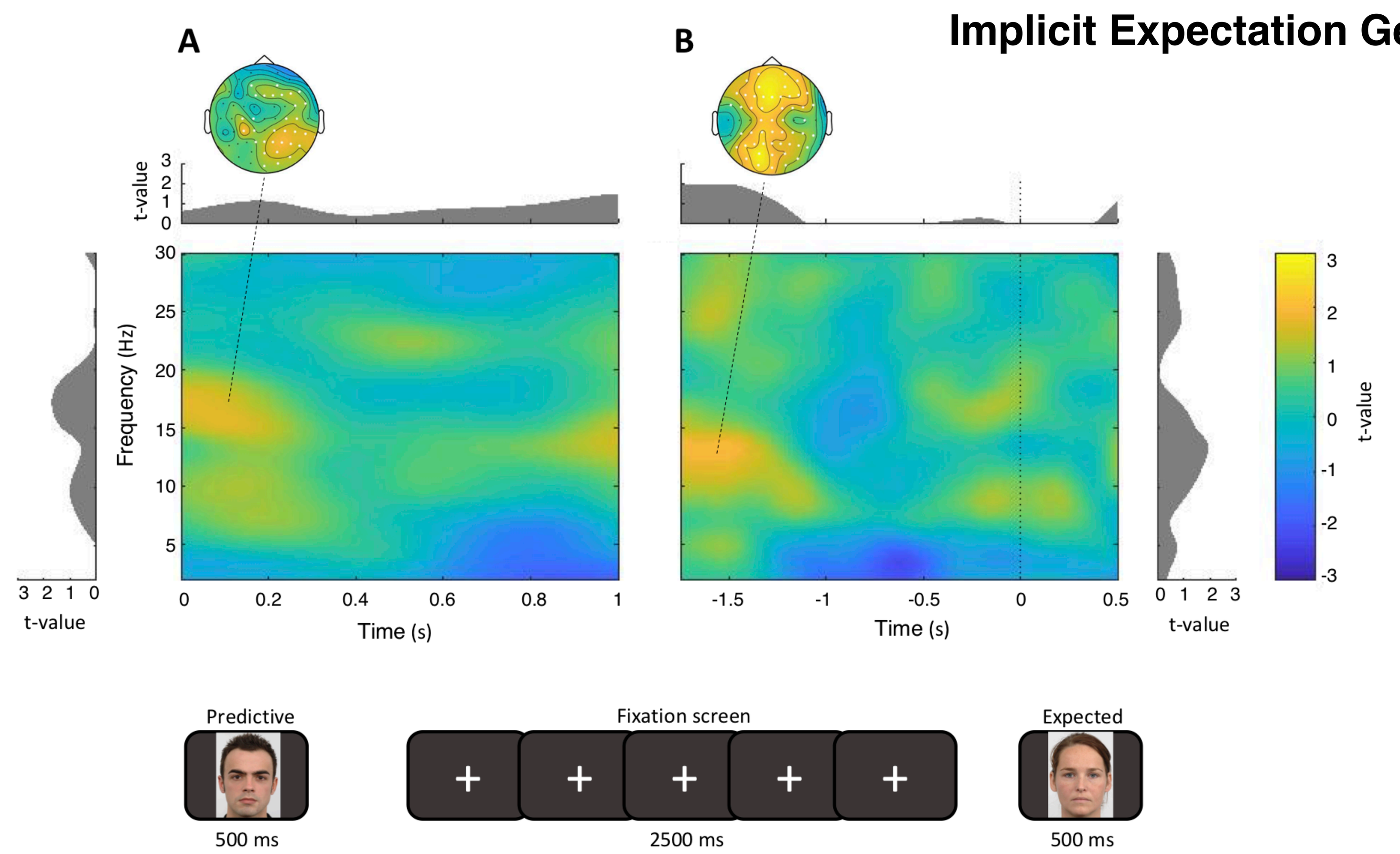

Figure 5. Differences in low-frequency power (2 – 30 Hz) averaged across all channels. **(A)** TFR illustrates the power differences (t-values) between the predictive and random images within the immediate, post-stimulus timeframe. The scalp topography shows the channels (highlighted in white) which correspond to the positive cluster (~ 0 – 0.2 s) within the frequency range of 15 – 20 Hz (p = .03, cluster corrected). Time is expressed relative to the onset of the predictive image. The margin graphs present the t-values for both time and frequency centred around 17 Hz. **(B)** TFR illustrates the power differences between the expected and random images leading up to stimulus onset. The topography reveals channels corresponding to the positive cluster which extends from approximately -1.75 to -1.45 s and 10 – 15 Hz (p = .008, cluster corrected). Time is expressed relative to the expected image onset. The margin graphs present the t-values for both time and frequency centred around 13 Hz.

Discussion

1. **No significant decrease in response time nor an increase in accuracy was evident for expected face images.**
   - Ceiling effect: The simplicity and repetitiveness of the task could have permitted participants to quickly reach optimal proficiency.
2. **A significant amplitude reduction in the N170 was evident over the left hemisphere.**
   - The left-lateralised reduction substantiates that participants had gained implicit knowledge of the predictive nature underlying the task[2].
   - Neural adaptation: Since the occurrences of all images were identical throughout the experiment, the insignificance of a right-lateralised reduction could be educed by confounding familiarity (predominantly found over the right-hemisphere)[10].
3. **Significant increase in GBA post-stimulus onset for statistically random face images.**
   - Enhancement in GBA is an indicator that the processing of random images is primarily dominated by bottom-up directed information flow[8].
4. **Significant increase in alpha/beta power prior to the onset of expected face images.**
   - The predictive image seems pivotal for the initiation of expectation genesis which terminates shortly prior to the onset of the expected image.
   - Expectations were subjected to alpha modulations (Fig. 5B), which efficiently prioritised top-down prediction projection whilst suppressing the forward flow of gamma facilitated prediction errors once the expected faces appeared[6,7].

References

1. Turk-Browne NB, Scholl BJ, Johnson MK, Chun MM (2010). J Neurosci 30: 11177-87.
2. Ran G, Zhang Q, Chen X, Pan Y (2014). PloS One 9: e114011.
3. Bauer M, Stenner MP, Friston KJ, Dolan RJ (2014). J Neurosci 34: 16117–25.
4. Cao L, Thut G, Gross J (2017). NeuroImage 147: 895–903.
5. Spaak E, Fonken Y, Jensen O, de Lange FP (2016). Cereb Cortex 26: 4327–36.
6. Gordon N, Tsuchiya N, Koenig-Robert R, Hohwy J (2019). PLoS Biol 17: e3000233.
7. Smout CA, Tang MF, Garrido, MI, Mattingley JB (2019). PLoS Biol 17: e2006812.
8. Bastos AM, Vezoli J, Bosman CA, Schoffelen JM, Oostenveld R, Dowdall JR, Fries P (2015). Neuron 85: 390–401.
9. Langner O, Dotsch R, Bijlstra G, Wigboldus DHJ, Hawk ST, van Knippenberg A (2010). Cogn Emot 24: 1377–88.
10. Jemel B, Schuller AM, Goffaux V (2010). J Cogn Neurosci 22: 2289–2305.

living.knowledge
WWU Münster